THE ASTROPHYSICAL JOURNAL, 494:13–19, 1998 February 10

COSMOLOGICAL REDSHIFT DISTORTION: DECELERATION, BIAS, AND DENSITY PARAMETERS FROM FUTURE REDSHIFT SURVEYS OF GALAXIES

TAKAHIRO T. NAKAMURA,[1] TAKAHIKO MATSUBARA,[2] AND YASUSHI SUTO[2]
Received 1997 May 28; accepted 1997 September 2

ABSTRACT

The observed two-point correlation functions of galaxies in redshift space become anisotropic because of the geometry of the universe, as well as because of the presence of the peculiar velocity field. On the basis of linear perturbation theory, we expand the induced anisotropies of the correlation functions with respect to the redshift z and obtain analytic formulae to infer the deceleration parameter q_0, the density parameter Ω_0, and the derivative of the bias parameter $d\ln b/dz$ at $z = 0$ in terms of the observable statistical quantities. The present method does not require any assumption of the shape and amplitude of the underlying fluctuation spectrum and thus can be applied to future redshift surveys of galaxies, including the Sloan Digital Sky Survey.

We also evaluate quantitatively the systematic error in estimating the value of $\beta_0 \equiv \Omega_0^{0.6}/b$ from a galaxy redshift survey on the basis of a conventional estimator for β_0, which neglects both the geometrical distortion effect and the time evolution of the parameter $\beta(z)$. If the magnitude limit of the survey is as faint as 18.5 (in B band) as in the case of the Sloan Digital Sky Survey, the systematic error ranges between -20% and 10% depending on the cosmological parameters. Although such systematic errors are smaller than the statistical errors in the current surveys, they will definitely dominate the expected statistical error for future surveys.

Subject headings: cosmology: theory — galaxies: distances and redshifts — large-scale structure of the universe — methods: statistical

1. INTRODUCTION

The volume of the current galaxy redshift surveys is steadily increasing. The Las Campanas redshift survey (Shectman et al. 1996), for example, has reached a median redshift of $z \sim 0.1$ and the number of galaxies is about 25,000. In the near future, the Sloan Digital Sky Survey (SDSS; e.g., Gunn & Weinberg 1995) will complete a spectroscopic survey of $\sim 10^6$ galaxies brighter than 18 mag over π steradians. The main purpose of this paper is to stress that in interpreting observational results from these huge surveys, geometrical and evolutionary effects that are intrinsic to nonzero redshifts become important since observations are performed not on the constant time hypersurface but on the light cone.

It is supposed that global isotropy and homogeneity of the universe guarantee the isotropy of the two-point correlation function of galaxies in *real* space (i.e., the correlation function depends only on the separation of galaxy pairs). In reality, however, the deviation from the pure Hubble flow or the peculiar velocity field induces anisotropy in the observed correlation function in *redshift* space (Davis & Peebles 1983; Kaiser 1987). This redshift-space distortion of the correlation function has been examined extensively in the literature both theoretically and observationally in order to infer the value of $\beta_0 = \Omega_0^{0.6}/b$ (Hamilton 1992; for a review, see Strauss & Willick 1995), where Ω_0 and b are the density and bias parameters, respectively.

If the redshift z becomes substantially larger than 0, the geometry of the universe itself becomes an additional source for the anisotropy in the two-point correlation functions (cosmological redshift distortion): an intrinsically spherical object in real space is elongated to an ellipse of axial ratio $H(z):z/S(z)$ along the line of sight in redshift space (Alcock & Paczyński 1979; Ryden 1995), where $H(z)$ is the Hubble parameter at z and $S(z)$ is the angular size distance (eqs. [5] and [6]). Ballinger, Heavens, & Peacock (1996) and Matsubara & Suto (1996) developed an idea to probe Ω_0 and the cosmological constant, λ_0, using this geometrical distortion in the correlation function, having quasar and/or galaxy clustering at high $z \gtrsim 1$ implicitly in mind. Two potential disadvantages of their methods are that they have to assume a specific shape of the fluctuation spectra of the objects before carrying out the analysis to find the best-fit values of Ω_0 and λ_0 and that the statistical errors as a result of the limited number of high-z objects hampers the precise determination of the cosmological parameters.

In this paper, we explore a possibility of using a sample of galaxy redshift surveys at $z < 1$. Although the geometrical distortion effect becomes less important at $z < 1$, the number of galaxies available for the statistical analysis in a given redshift bin is larger by 2 orders of magnitude than high-z quasars, which compensates at least partially the weak signal at $z < 1$. In addition, we are successful in evaluating the degree of the cosmological redshift distortion both *analytically* and *independently* of the underlying fluctuation spectrum shape by expanding the cosmological distortion effect up to linear order in z and using linear density perturbation. Specifically, we propose in § 3 a method of determining the deceleration parameter q_0, as well as Ω_0 and $d\ln b/dz|_{z=0}$, in this way, which would be possible if the correlation function anisotropy can be accurately measured on large scales where linear density perturbation theory applies. Our expansion also enables us to estimate quantitatively how the value of β_0 determined from Hamilton's (1992) method systematically deviates from its true value

[1] Department of Physics, University of Tokyo, Tokyo 113, Japan; nakamura@utaphp2.phys.s.u-tokyo.ac.jp.
[2] Department of Physics, University of Tokyo, Tokyo 113, Japan; and Research Center for the Early Universe, University of Tokyo, Tokyo 113, Japan; matsu@phys.s.u-tokyo.ac.jp, suto@phys.s.u-tokyo.ac.jp.

because of the neglect of the geometrical effect at $z \neq 0$. In § 4 we show that systematic errors are smaller than the statistical errors in the current surveys but that they should dominate the expected statistical error for future surveys. Section 2 summarizes our notation, which is extensively used throughout the paper. Summary and conclusions are given in § 5. We use the units in which c and H_0 are unity.

2. NOTATION

Consider two nearby galaxies located at a redshift of z with a small redshift separation Δz ($\ll z$) and angular separation $\Delta\theta$ on the sky. The separation between them, s, and the direction cosine along the line of sight, v, in the observable (redshift space) coordinates are

$$s = [(\Delta z)^2 + (z\Delta\theta)^2]^{1/2} , \tag{1}$$

$$v = \Delta z/s , \tag{2}$$

while those in the comoving coordinates are

$$r = \{[\Delta z/H(z)]^2 + [S(z)\Delta\theta]^2\}^{1/2} , \tag{3}$$

$$\mu = [\Delta z/H(z)]/r , \tag{4}$$

where

$$H(z) = [\Omega_0(1+z)^3 - K(1+z)^2 + \lambda_0]^{1/2} \tag{5}$$

is the Hubble parameter at z, $K = \Omega_0 + \lambda_0 - 1$,

$$S(z) = \begin{cases} K^{-1/2} \sin (K^{1/2}\chi) & (K > 0) \\ \chi & (K = 0) \\ (-K)^{-1/2} \sinh [(-K)^{1/2}\chi] & (K < 0) \end{cases} \tag{6}$$

is the angular size distance (e.g., Peebles 1993) from us to z, and

$$\chi(z) = \int_0^z dz'/H(z') . \tag{7}$$

The peculiar motions of galaxies induce anisotropy in the two-point correlation function $\xi_s(s, v; z)$ in redshift space (Kaiser 1987), while the real-space correlation function $\xi(r; z)$ is isotropic (i.e., independent of the direction cosine μ). Hamilton (1992) expanded the redshift-space correlation function on the basis of linear theory of density perturbation and distant-observer approximation in terms of the Legendre polynomials with respect to the direction cosine μ along the line of sight at $z = 0$ where (s, v) and (r, μ) coincide. Matsubara & Suto (1996) showed that Hamilton's formula can be generalized to the $z \neq 0$ case even if the cosmological distortion effect is taken into account:

$$\xi_s(s, v; z) = \sum_{l=0}^{2} \xi_{2l}(r; z) P_{2l}(\mu) , \tag{8}$$

where (s, v) and (r, μ) are related to each other by equations (1)–(4), and the expansion coefficients are explicitly given in terms of the real-space correlation function of galaxies $\xi(r; z)$ as follows:

$$\xi_0(r; z) = [1 + \tfrac{2}{3}\beta(z) + \tfrac{1}{5}\beta^2(z)]\xi(r; z) , \tag{9}$$

$$\xi_2(r; z) = [\tfrac{4}{3}\beta(z) + \tfrac{4}{7}\beta^2(z)]\xi_d(r; z) , \tag{10}$$

$$\xi_4(r; z) = \tfrac{8}{35}\beta^2(z)[\xi_d(r; z) + \tfrac{7}{2}\xi_q(r; z)] , \tag{11}$$

$$\xi_d(r; z) = \xi(r; z) - 3\int_0^r \frac{dx}{x}\left(\frac{x}{r}\right)^3 \xi(x; z) , \tag{12}$$

$$\xi_q(r; z) = \int_0^r \frac{dx}{x}\left[3\left(\frac{x}{r}\right)^3 - 5\left(\frac{x}{r}\right)^5\right]\xi(x; z) . \tag{13}$$

The β parameter is defined as $\beta(z) = f(z)/b(z)$, with the bias parameter b and the following functions

$$f(z) = \frac{d\ln D}{d\ln a} = \frac{[(1+z)/H(z)]^2}{D(z)} - [1 + q(z)] \tag{14}$$

$$\simeq \Omega^{0.6}(z) + \tfrac{1}{70}\lambda(z)[1 + \tfrac{1}{2}\Omega(z)] , \tag{15}$$

$$D(z) = H(z)\int_z^\infty dz'(1+z')/H^3(z') , \tag{16}$$

$$q(z) = -\frac{d\ln H}{d\ln a} - 1 = \frac{1}{2}\Omega(z) - \lambda(z) , \tag{17}$$

$$\Omega(z) = \Omega_0(1+z)^3/H^2(z) , \quad \lambda(z) = \lambda_0/H^2(z) \tag{18}$$

(e.g., Peebles 1980; Lahav et al. 1991). Defining

$$X(r; z) = \left[\xi_0(r; z) - 3\int_0^1 dx\, x^2 \xi_0(rx; z)\right] \Big/ \xi_2(r; z) \tag{19}$$

(Hamilton 1992), one finds from equations (9) and (10) that

$$\beta(z) = \tfrac{3}{2}/[X - \tfrac{1}{2} + (X^2 + \tfrac{2}{7}X - \tfrac{1}{5})^{1/2}] . \tag{20}$$

3. MEASURING THE DECELERATION PARAMETER FROM REDSHIFT DISTORTION AT SMALL REDSHIFTS

Matsubara & Suto (1996) showed that the shape of contour curves of $\xi_s(s, v; z)$ at $z \gtrsim 1$ sensitively depends on Ω_0 and λ_0 and proposed to test the nonvanishing λ_0 in particular by comparing theoretical prediction with observation. As mentioned in § 1, however, this method is model dependent in the sense that such a determination of Ω_0 and λ_0 is possible only when one assumes a priori a specific power spectrum, such as that of the cold dark matter (CDM) model, in order to fix the (unobservable) real-space correlation function $\xi(r; z)$. This is because the comoving coordinates (r, μ) themselves depend on Ω_0 and λ_0 at $z \neq 0$ (eqs. [3] and [4]): one cannot extract the multipole components ξ_{2l} directly from the observed correlation function ξ_s (eq. [8]) without a priori knowledge of Ω_0 and λ_0, but rather the observed ξ_s needs to be compared with the one calculated theoretically from equation (8) with an assumed model power spectrum. Thus, $\xi_{2l}(r; z)$ are not directly observable quantities at $z \neq 0$, but the observable ones should be expressed in terms of the redshift-space variables like

$$\zeta_{2l}(s; z) = (2l + \tfrac{1}{2})\int_{-1}^{1} dv P_{2l}(v)\xi_s(s, v; z) , \tag{21}$$

i.e., the multipole expansion with respect to the observable coordinate v instead of μ [note that $\zeta_{2l}(s; 0) = \xi_{2l}(r; 0)$].

In this sense, it is desirable to rewrite equation (8) entirely in terms of $\zeta_{2l}(s; z)$ and $P_{2l}(v)$, but this expansion has an infinite number of terms. However, we find that this expansion becomes finite if all the variables are expanded up to linear order in z. This perturbation analysis is quite relevant since we have specifically in mind the SDSS galaxy redshift survey ($z \lesssim 0.2$) throughout the present paper. With this prescription, we obtain explicit expressions for the deceleration parameter q_0, the density parameter Ω_0, and the derivative of the bias parameter $d\ln b/dz$ at $z = 0$ in terms of the observable quantities. As shown below, the advantage

of the present method is that the resulting formulae are written only in terms of the observables and independent of the model power spectrum, unlike the high-z analysis (Matsubara & Suto 1996).

To linear order in z, (r, μ) and (s, v) are written from equations (1)–(4) as

$$r \simeq [1 - \tfrac{1}{2}(1 + v^2)(1 + q_0)z]s \,, \tag{22}$$

$$\mu \simeq [1 - \tfrac{1}{2}(1 - v^2)(1 + q_0)z]v \,, \tag{23}$$

where throughout we use the symbol $\simeq$ to indicate that the equality is valid only up to linear order in z. Substituting these into equation (8) and using equation (21), we obtain

$$\xi_s(s, v; z) \simeq \sum_{l=0}^{3} \zeta_{2l}(s; z) P_{2l}(v) \,, \tag{24}$$

$$\zeta_0(s; z) \simeq \xi_0(s; z) - \frac{2}{3}\left(1 + \frac{4}{5}\beta_0 + \frac{9}{35}\beta_0^2\right) \times \frac{\partial \xi(s; 0)}{\partial \ln s}(1 + q_0)z \,, \tag{25}$$

$$\zeta_2(s; z) \simeq \xi_2(s; z) + \left[\left(\frac{20}{7}\beta_0 + \frac{4}{3}\beta_0^2\right)\xi_d(s; 0) - \frac{1}{3}\left(1 + \frac{26}{7}\beta_0 + \frac{11}{7}\beta_0^2\right)\frac{\partial \xi(s; 0)}{\partial \ln s}\right](1 + q_0)z \,, \tag{26}$$

$$\zeta_4(s; z) \simeq \xi_4(s; z) + \left[\left(\frac{8}{7}\beta_0 + \frac{24}{11}\beta_0^2\right)\xi_d(s; 0) + \frac{32}{11}\beta_0^2 \xi_q(s; 0) - \frac{8}{35}\left(\beta_0 + \frac{13}{11}\beta_0^2\right)\frac{\partial \xi(s; 0)}{\partial \ln s}\right](1 + q_0)z \,, \tag{27}$$

$$\zeta_6(s; z) \simeq \frac{4}{33}\beta_0^2 \times \left[4\xi_d(s; 0) + 9\xi_q(s; 0) - \frac{2}{7}\frac{\partial \xi(s; 0)}{\partial \ln s}\right](1 + q_0)z \,, \tag{28}$$

where $\beta_0 = \beta(0)$. Equations (25)–(28) represent the geometrical effect on the redshift-space distortion of the correlation function to linear order in z. We also calculate its time evolution for consistency:

$$\xi_0(s; z) \simeq \xi_0(s; 0) - z[(1 + \tfrac{1}{3}\beta_0)\phi_0 + (\tfrac{1}{3}\beta_0 + \tfrac{1}{5}\beta_0^2)\psi_0]\xi(s; 0) \,, \tag{29}$$

$$\xi_2(s; z) \simeq \xi_2(s; 0) - z[\tfrac{2}{3}\beta_0\phi_0 + (\tfrac{2}{3}\beta_0 + \tfrac{4}{7}\beta_0^2)\psi_0]\xi_d(s; 0) \,, \tag{30}$$

$$\xi_4(s; z) \simeq (1 - \psi_0 z)\xi_4(s; 0) \,, \tag{31}$$

where

$$\phi_0 = -\frac{d}{dz}\ln|\xi|\bigg|_{z=0} = 2f_0 - 2\frac{d}{dz}\ln b\bigg|_{z=0} \,, \tag{32}$$

$$\psi_0 = -\frac{d}{dz}\ln|\beta^2\xi|\bigg|_{z=0} = \frac{3\Omega_0}{f_0} - 2(1 - q_0) \tag{33}$$

(the subscript 0 denotes variables at the present epoch $z = 0$). In the second equality of equations (32) and (33), it is assumed that the real-space correlation function $\xi(r; z)$ evolves as $\propto [b(z)D(z)]^2$ with z. Note that ψ_0 measures the time evolution of the velocity correlation.

Next we integrate the observable quantities $[\xi_{2l}(s; 0) - \zeta_{2l}(s; z)]/z$ over s with some appropriate weights and eliminate the derivative terms $\partial\xi/\partial \ln s$ in equations (25)–(28). Performing three such integrals, we obtain linear equations of the form

$$\begin{bmatrix} c_{11} & c_{12} & c_{13} \\ c_{21} & c_{22} & c_{23} \\ c_{31} & c_{32} & c_{33} \end{bmatrix}\begin{bmatrix} 1 + q_0 \\ \phi_0 \\ \psi_0 \end{bmatrix} \simeq \begin{bmatrix} d_1 \\ d_2 \\ d_3 \end{bmatrix} , \tag{34}$$

where d_i are the integrals of $[\xi_{2l}(s; 0) - \zeta_{2l}(s; z)]/z$ (an explicit set of examples is given by eqs. [35]–[37]) and c_{ij} consist of β_0 and $\xi(r; 0)$. If we assume that c_{ij} are known from observation at $z \sim 0$, then we can infer the values of $1 + q_0$, ϕ_0, and ψ_0 by solving equation (34) with respect to them. In this way, the cosmological parameters, as well as (local) evolution of the bias, can be determined in principle, without assuming any specific cosmological models such as CDM, by observing the multipole components $\zeta_{2l}(s; z)$ at small z.

The sixth moment ζ_6, which does not appear in Hamilton's formula at $z = 0$, shows up in our expansion in redshift space at $z \neq 0$ (within the linear density perturbation), and according to equation (25), the solution for $1 + q_0$ has a rather simple form in terms of an integral of ζ_6. However, higher-order moments would become progressively difficult to be determined reliably and also are likely to be contaminated by nonlinear effects (Cole, Fisher, & Weinberg 1994, 1995). Therefore. we eliminate the use of the sixth-order moment and find that the following choice of d_i leads to the simplest form of the solution for $1 + q_0$ among what we have examined:

$$d_1(s; z) = \int_0^1 dx(3x^2 - 5x^4)[\xi_0(sx; 0) - \zeta_0(sx; z)]/z \,, \tag{35}$$

$$d_2(s; z) = 3\int_0^1 dx\, x^4[\xi_2(sx; 0) - \zeta_2(sx; z)]/z \,, \tag{36}$$

$$d_3(s; z) = \tfrac{35}{4}\int_0^1 dx\, x[\xi_4(s/x; 0) - \zeta_4(s/x; z)]/z \,. \tag{37}$$

Then it follows from equations (25)–(31) that

$$c_{11}(s) = -\tfrac{2}{3}(1 + \tfrac{4}{5}\beta_0 + \tfrac{9}{35}\beta_0^2)[2\xi_d(s; 0) + 5\xi_q(s; 0)] \tag{38}$$

$$c_{12}(s) = (1 + \tfrac{1}{3}\beta_0)\xi_q(s; 0) \,, \tag{39}$$

$$c_{13}(s) = (\tfrac{1}{3}\beta_0 + \tfrac{1}{5}\beta_0^2)\xi_q(s; 0) \,, \tag{40}$$

$$c_{21}(s) = (1 + \tfrac{26}{7}\beta_0 + \tfrac{11}{7}\beta_0^2)\xi_d(s; 0) + (1 + 8\beta_0 + \tfrac{25}{7}\beta_0^2)\xi_q(s; 0) \,, \tag{41}$$

$$c_{22}(s) = -\beta_0 \xi_q(s; 0) \,, \tag{42}$$

$$c_{23}(s) = -(\beta_0 + \tfrac{6}{7}\beta_0^2)\xi_q(s; 0) \,, \tag{43}$$

$$c_{31}(s) = -2(\beta_0 + \tfrac{13}{11}\beta_0^2)\xi_d(s; 0) - \tfrac{40}{11}\beta_0^2 \xi_q(s; 0) \,, \tag{44}$$

$$c_{32} = 0 \,, \tag{45}$$

$$c_{33}(s) = \beta_0^2\,\xi_q(s;\,0)\,. \tag{46}$$

From equations (38)–(46), we solve equation (34) for $1 + q_0$ as

$$1 + q_0 \simeq \beta_0^2\,\frac{d_1}{\Delta} + \left(\beta_0 + \frac{1}{3}\,\beta_0^2\right)\frac{d_2}{\Delta} + \left(1 + \frac{6}{7}\,\beta_0 + \frac{3}{35}\,\beta_0^2\right)\frac{d_3}{\Delta}\,, \tag{47}$$

where

$$\Delta(s) = (\beta_0 + \tfrac{15}{11}\beta_0^2 + \tfrac{5}{11}\beta_0^3 + \tfrac{5}{231}\beta_0^4)[\xi_q(s;\,0) - \xi_d(s;\,0)]\,, \tag{48}$$

and d_1, d_2, and d_3 are defined in equations (35)–(37). The solutions for ϕ_0 and ψ_0 (eqs. [32] and [33]) are presented in the Appendix.

Figure 1 illustrates the extent to which equation (47) is useful in determining q_0, where we plot the inferred value q_* of q_0 (left-hand side of eq. [47]) versus β_*, which is substituted for β_0 in the right-hand sides of equations (47) and (48) for three representative sets of Ω_0 and λ_0 assuming $\beta_0 = 0.5$ in all cases. In the figure we calculate ξ_{2l} and ζ_{2l} from equations (8) and (21) assuming that b is constant and $\xi(r;\,z) \propto D^2(z)$. The integrals in equations (35)–(37) are performed numerically over $0.01 < x < 1$ in logarithmic interval. The real-space correlation function $\xi(r;\,0)$ is calculated from the scale-invariant ($n = 1$) CDM-like power spectrum in Bardeen et al. (1986) with the shape parameter $\Gamma = 0.25$ irrespective of (Ω_0, λ_0), since the spectrum with these parameters fits the observed linear power spectrum fairly well (Peacock & Dodds 1994). The crosses show the true value of $q_0 = \frac{1}{2}\Omega_0 - \lambda_0$ for each (Ω_0, λ_0). The three curves for each model correspond to the $z = 0.01$, 0.1, and 0.2 cases, with smaller z corresponding to the curve nearer to the crosses.

To determine q_0 in practice, one would probably bin the observational data in z with the width of $\Delta z \ll z$, calculate the multipole components of the correlation function anisotropy within each bin, and substitute them for $\xi_{2l}(s;\,0)$ and $\zeta_{2l}(s;\,z)$ in equations (35)–(37). Since these equations contain subtractions of two similar quantities, one needs very accurate data of them to avoid round-off errors. Thus, the actual curve drawn from observation may have very large error bars, so a sample as large as the SDSS catalog is required for that purpose. Also, one has to guess the trial value β_* of β_0 from observation at $z \sim 0$.

The curves in the figure do not pass exactly through the crosses since we have neglected terms of order z^2, so the deviations of the curves from the crosses represent the second-order contributions. Alternatively, by extrapolating the curves to $z \sim 0$, one may infer a curve on which the true q_0 lies. The z-dependence is very large for the Einstein–de Sitter ($\Omega_0 = 1$ and $\lambda_0 = 0$) model, and one may not be able to distinguish the Einstein–de Sitter and open ($\Omega_0 = 0.2$ and $\lambda_0 = 0$) models. We expect, however, that $\lambda_0 = 0$ and $\lambda_0 \sim 1$ models can be distinguished clearly. Moreover, unlike the Einstein–de Sitter and open models, the curve in the Λ model ($\Omega_0 = 0.2$ and $\lambda_0 = 0.8$) is quite insensitive to the value of β_*, implying that q_0 may be inferred very reliably even if the uncertainty in the estimate of β_0, i.e., $\beta_* - \beta_0$, is fairly large.

Figures 2 and 3 show the same plots for ϕ_0 and ψ_0 (eqs. [32] and [33]) as in Figure 1, using equations (A3)–(A8). We expect that ϕ_* can distinguish high-Ω_0 and low-Ω_0 models [if the bias $b(z)$ does not evolve] and ψ_* can distinguish all the three models. Thus, one can put strong constraints on Ω_0, λ_0, and β_0 by combining the three inferred quantities

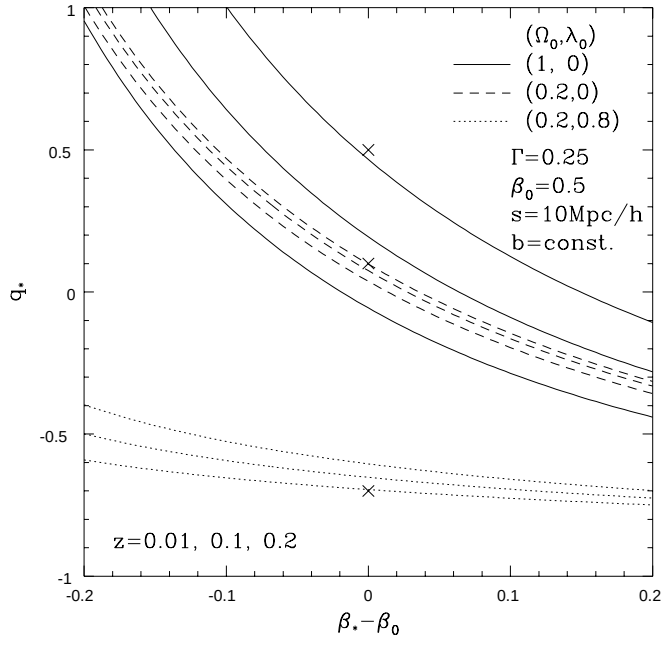

FIG. 1.—Inferred value q_* of the deceleration parameter q_0 from eq. (47), vs. β_*, which is substituted for $\beta_0 = \Omega_0^{0.6}/b$ in the right-hand sides of eqs. (47) and (48). The crosses indicate the location of the true values of $q_0 = \frac{1}{2}\Omega_0 - \lambda_0$. The three curves for each model correspond to the $z = 0.01$, 0.1, and 0.2 cases, with smaller z corresponding to the curve nearer to the crosses.

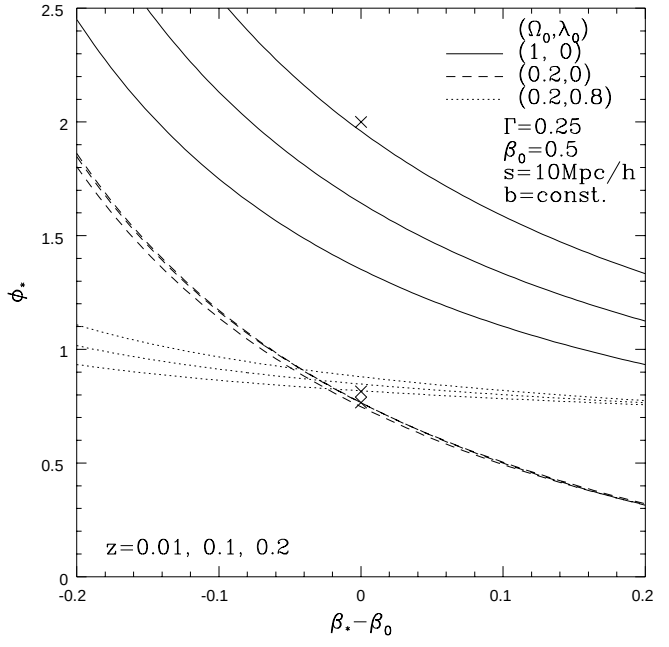

FIG. 2.—Same as Fig. 1, on $\phi_0 = 2\Omega_0^{0.6} - 2d\ln b/dz\,|_{z=0}$ (see eqs. [32] and [A1]).

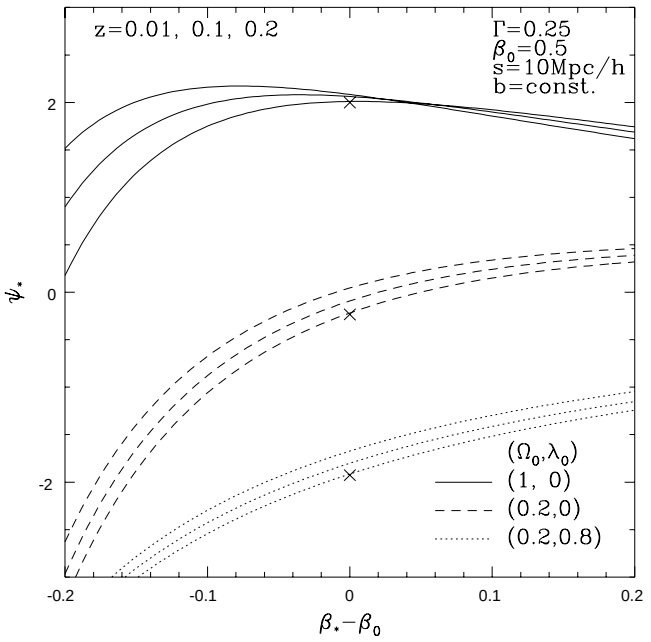

FIG. 3.—Same as Fig. 1, on $\psi_0 = 3\Omega_0^{0.4} - 2(1 - q_0)$ (see eqs. [33] and [A2]).

q_*, ϕ_*, and ψ_*. If one determines these parameters with the above methods, then Ω_0, λ_0, and the evolution of bias $d \ln b/dz|_{z=0}$ can also be determined in principle, since these have a one-to-one correspondence with q_0, ϕ_0, and ψ_0.

4. GEOMETRICAL AND EVOLUTIONARY EFFECTS ON THE ESTIMATES OF β_0

As noted in the last section, the directly observable quantities are not the multipole components ξ_{2l} but ζ_{2l}. Thus, equation (20) is useful only at $z \sim 0$ to infer the value of $\beta_0 = \beta(0)$. In addition to the difference between μ and v, the time-evolution of both the peculiar velocity field and the bias also affects the estimates of β_0. Therefore, as the depth of the redshift survey increases, the value of β_0 estimated from equation (20) in a straightforward manner would deviate systematically from the true value.

The systematic deviation $\Delta\beta$ as a function of z can be evaluated by substituting the observable ζ_{2l} with ξ_{2l} in equation (19):

$$Z(s; z) = \left[\zeta_0(s; z) - 3\int_0^1 dx\, x^2 \zeta_0(sx; z)\right] \Big/ \zeta_2(s; z) . \quad (49)$$

The resulting estimator of the β-parameter according to equation (20) is

$$\begin{aligned}\beta_{\rm obs}(z) &= \tfrac{3}{2}/[Z - \tfrac{1}{2} + (Z^2 + \tfrac{2}{7}Z - \tfrac{1}{5})^{1/2}] \\ &= \beta_0 + \Delta\beta_{\rm evol}(z) + \Delta\beta_{\rm geom}(z) , \end{aligned} \quad (50)$$

where we define

$$\Delta\beta_{\rm evol}(z) = \beta(z) - \beta_0 , \quad (51)$$

$$\Delta\beta_{\rm geom}(z) = \beta_{\rm obs}(z) - \beta(z) . \quad (52)$$

The former correction term $\Delta\beta_{\rm evol}$ simply represent the time evolution of both the velocity field and the bias, while the latter term arises from the geometrical effect that we have discussed. Using equations (25)–(31), these are expressed up to linear order in z as

$$\Delta\beta_{\rm evol}(z) \simeq \left.\frac{d\beta}{dz}\right|_{z=0} z = \frac{1}{2}\beta_0(\phi_0 - \psi_0)z , \quad (53)$$

$$\begin{aligned}\Delta\beta_{\rm geom}(z) \simeq\ & -(1 + q_0)z \Big/ \left(1 + \frac{6}{7}\beta_0 + \frac{3}{35}\beta_0^2\right) \\ & \times \left[\frac{1}{4}\left(1 + \frac{12}{7}\beta_0 + \frac{34}{35}\beta_0^2 + \frac{4}{21}\beta_0^3 + \frac{1}{49}\beta_0^4\right)\right. \\ & \times \left(3 + \left.\frac{\partial \ln|\xi_d|}{\partial \ln s}\right|_{z=0}\right) \\ & \left. - \frac{1}{7}\left(\beta_0 - \frac{1}{5}\beta_0^2 - \frac{11}{35}\beta_0^3 - \frac{1}{7}\beta_0^4\right)\right] . \end{aligned} \quad (54)$$

Figure 4 plots $\Delta\beta(z)$ for three sets of values of (Ω_0, λ_0), again assuming $\beta_0 = 0.5$. Thin and thick curves correspond to $\Delta\beta_{\rm evol}$ (eq. [51]) and $\Delta\beta_{\rm evol} + \Delta\beta_{\rm geom}$ (eq. [52]), respectively. In the figure we set the bias parameter b to be constant with z, so $\beta(z) \propto f(z)$. As in Figures 1–3, $\zeta_{2l}(s)$ were calculated from equations (8) and (21), using the CDM-like power spectrum of $\Gamma = 0.25$ and $n = 1$ (see § 3). The integral in equation (49) was performed numerically over $0.01 < x < 1$ using bins with the logarithmically equal interval.

As seen from Figure 4 and equations (53) and (54), $\Delta\beta_{\rm evol}$ and $\Delta\beta_{\rm geom}$ are generally positive and negative, respectively; for $\lambda_0 = 0$ models, the geometrical effect (proportional to $1 + q_0$) is important and dominates the evolutionary effect so that the total $\Delta\beta$ is negative. On the contrary, the

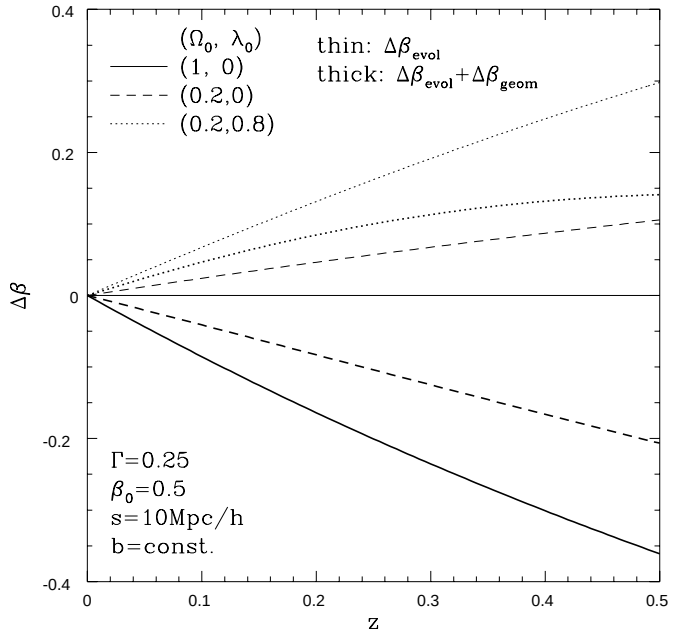

FIG. 4.—Systematic deviation $\Delta\beta$ in the estimates of $\beta_0 = \Omega_0^{0.6}/b$ vs. redshift. Thin and thick curves correspond to $\Delta\beta_{\rm evol}$ (eq. [51]) and $\Delta\beta_{\rm evol} + \Delta\beta_{\rm geom}$ (eq. [52]), respectively.

opposite is true for $\lambda_0 \sim 1$ models because of the steady character of the de Sitter spacetime, so $\Delta\beta$ is positive. In all the models in Figure 4, the systematic deviation $\Delta\beta$ amounts to more than 10% beyond the redshift of 0.1.

To be more realistic, the multipole components obtained from actual redshift survey (whose limiting magnitude is m) may be written as an average over the redshift:

$$\langle \zeta_{2l}(s; m) \rangle = \int_0^\infty dz\, w(z)\, \zeta_{2l}(s; z)\ . \tag{55}$$

The weight function $w(z)$, with the normalization $\int_0^\infty dz\, w(z) = 1$, is contributed from the survey volume and the selection for galaxy brightness:

$$w(z) = [S^2(z)/H(z)] \int_{L(z)}^\infty \Phi(L')\, dL'\ , \tag{56}$$

$$L(z) = 4\pi[(1 + z)S(z)]^2 f_{\min}\ , \tag{57}$$

where $\Phi(L)dL$ is the galaxy luminosity function and $f_{\min}$ is the faintest flux corresponding to the limiting magnitude m. Substituting $\langle \zeta_{2l}(s; m) \rangle$ instead of $\zeta_{2l}(s; z)$ in equation (49), we can estimate the systematic deviation $\Delta\beta(m) = \beta_{\rm obs}(m) - \beta_0$ in the estimates of β_0.

Figure 5 plots $\Delta\beta$ versus the limiting magnitude of surveys in B band. We adopt the parameters for the galaxy luminosity function from Loveday et al. (1992) and use the same cosmological parameters as in Figure 4. Incidentally, we perform the same calculation except that the correlation function is constant with z, i.e., $\xi(r; z) = \xi(r; 0)$, and find that little difference is shown compared with Figure 5. Thus, the results in Figure 5 do not depend on how the density contrast evolves with time.

The Durham/UKST redshift survey (Ratcliffe et al. 1996) and the Stromlo-APM redshift survey (Loveday et al. 1996) estimate that $\beta_0 = 0.55 \pm 0.12$ and 0.48 ± 0.12, respectively,

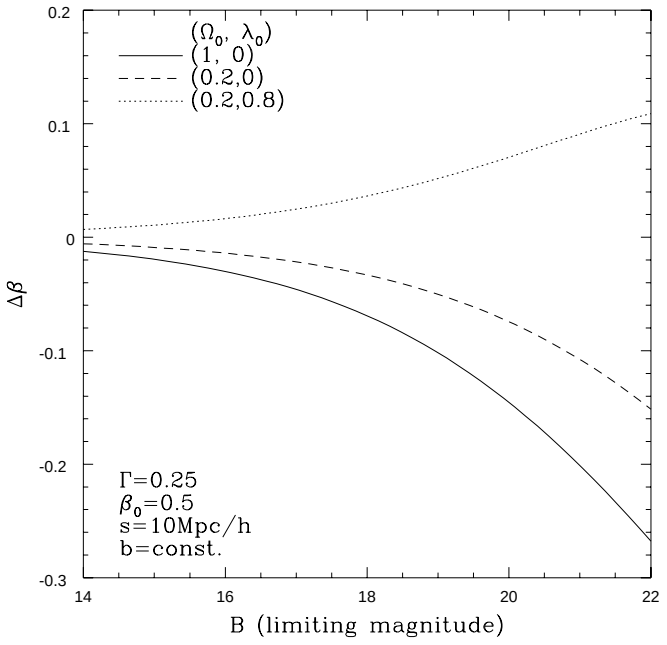

FIG. 5.—Systematic deviation $\Delta\beta$ in the estimates of $\beta_0 = \Omega_0^{0.6}/b$ vs. the limiting magnitude of redshift surveys in B band.

from $\sim 10^3$ galaxies of $B \lesssim 17$ mag. From Figure 5, the systematic deviation $\Delta\beta$ is less than ~ 0.05 (10%) for $B < 17$, which is smaller than the statistical error, ± 0.12. On the other hand, future redshift surveys of galaxies, the SDSS, for example, will observe $\sim 10^6$ galaxies with $B \lesssim 18.5$ (Fukugita, Shimasaku, & Ichikawa 1995). This huge number of galaxies should greatly reduce the statistical error in the estimates of β_0, and the systematic deviation pointed out in this paper should dominate the statistical errors.

5. SUMMARY AND CONCLUSION

In this paper we have shown that when interpreting observational results from forthcoming huge redshift surveys, it is necessary to consider geometrical and evolutionary effects that are intrinsic to nonzero redshifts, because of the fact that observations are performed on the light cone. With the geometrical and light-cone effects, the Hamilton's (1992) method of determining β_0 does not work in a straightforward manner. This is why Matsubara & Suto (1996) proposed the model-dependent comparison with observation. In fact, we are working on a method to determine cosmological parameters independently of the underlying fluctuation spectrum (T. Matsubara et al. 1998, in preparation). For $z \ll 1$, as we consider in the present paper, however, the straightforward application of the Hamilton method works in determining the parameters independently of the spectra, as we showed explicitly.

In § 3, we have explicitly obtained the expressions for the observable multipole components of the redshift-space correlation function up to linear order in the redshift, bearing specifically in mind the redshift survey data of $z < 1$ like the SDSS. Then we derived analytic formulae, in linear theory and the distant observer approximation, to infer the cosmological parameters q_0, ϕ_0, and ψ_0 (eqs. [32] and [33] for definition) in terms of these multipole components at small z. Assuming that $\beta_0 = \Omega_0^{0.6}/b$ and $\xi(r; 0)$ are independently given from observations at $z \sim 0$, our formulae (eqs. [47], [A1], and [A2]) provide model-independent determination of these parameters from observation of the redshift-space correlation function at small z. To determine them in practice, one would probably bin the observational data in z with the width of $\Delta z \ll z$, calculate the multipole components ζ_{2l} of the correlation function anisotropy within each bin, and substitute them in equations (35)–(37). Since these equations contain subtractions of two similar quantities, one needs very accurate data to avoid roundoff errors, so a sample as large as the SDSS catalog is required for that purpose. Also, one has to guess at the value of β_0 in the formulae from observation at $z \sim 0$. If one determines q_0, ϕ_0, and ψ_0 in this way, then Ω_0, λ_0, and the evolution of bias $d \ln b/dz|_{z=0}$ are also obtained.

In § 4, we pointed out that the value of β_0 estimated by existing methods deviates systematically from its true value, as a result of the time evolution of both the velocity field and the bias, and also as a result of the cosmological geometry. We quantitatively estimated the systematic deviation $\Delta\beta$ when Hamilton's formula (eq. [20]) is applied to data of large-scale redshift surveys and found that $\Delta\beta/\beta_0 \lesssim 10\%$ for $B < 17$ (Fig. 1), which is smaller than the statistical errors of currently estimated β_0 from existing surveys (Ratcliffe et al. 1996; Loveday et al. 1996). For the SDSS ($B < 18.5$; Fukugita et al. 1995), in which the statistical error is expected to be significantly reduced, we found

$\Delta\beta/\beta_0$ ranges between -20% and 10% depending on the cosmological parameters. Thus, the systematic deviation is likely to dominate the statistical error in the next generation deep and wide redshift surveys.

The remaining future work is to examine, using a mock sample from an N-body simulation, whether our formulae can practically be applied to determine the cosmological parameters. We plan to "observe" the redshift dependence of the multipole components ζ_{2l} in a mock sample like the SDSS, binning the N-body data in z (Magira et al. 1998, in preparation). At the same time, it is essential to work out more efficient and accurate ways of obtaining the multipole components from survey or mock data on large scales where linear theory applies and/or to include nonlinear effects in our analytic calculations.

We thank the referee, David Weinberg, for several useful comments on the earlier manuscript, which helped improve the presentation of the paper. T. T. N. gratefully acknowledges support from a JSPS (Japan Society of Promotion of Science) fellowship. This work is supported in part by grants-in-aid by the Ministry of Education, Science, Sports and Culture of Japan (4125, 07CE2002, 07740183).

APPENDIX

SOLUTIONS FOR ϕ_0 AND ψ_0

In terms of the integrals d_1, d_2, and d_3 (eqs. [35]–[37]), the solutions of equation (34) for ϕ_0 (eq. [32]) and ψ_0 (eq. [33]) are written as

$$\phi_0 \simeq (\Delta_{\phi 1}\, d_1 + \Delta_{\phi 2}\, d_2 + \Delta_{\phi 3}\, d_3)/\Delta\,, \tag{A1}$$

$$\psi_0 \simeq (\Delta_{\psi 1}\, d_1 + \Delta_{\psi 2}\, d_2 + \Delta_{\psi 3}\, d_3)/\Delta\,, \tag{A2}$$

where Δ is defined in equation (48) and

$$\Delta_{\phi 1}(s) = \beta_0 + \frac{48}{11}\,\beta_0^2 + \frac{5}{11}\,\beta_0^3 - \left(\beta_0 + \frac{4}{11}\,\beta_0^2 + \frac{5}{11}\,\beta_0^3\right)\frac{\xi_d(s;0)}{\xi_q(s;0)}\,, \tag{A3}$$

$$\Delta_{\phi 2}(s) = \frac{10}{3}\,\beta_0 + \frac{16}{11}\,\beta_0^2 + \frac{10}{77}\,\beta_0^3 + \left(\frac{2}{3}\,\beta_0 - \frac{4}{33}\,\beta_0^2 - \frac{10}{77}\,\beta_0^3\right)\frac{\xi_d(s;0)}{\xi_q(s;0)}\,, \tag{A4}$$

$$\Delta_{\phi 3}(s) = 3 + \frac{93}{35}\,\beta_0 + \frac{37}{105}\,\beta_0^2 + \frac{1}{49}\,\beta_0^3 + \left(1 + \frac{27}{35}\,\beta_0 - \frac{1}{105}\,\beta_0^2 - \frac{1}{49}\,\beta_0^3\right)\frac{\xi_d(s;0)}{\xi_q(s;0)}\,, \tag{A5}$$

$$\Delta_{\psi 1}(s) = \frac{40}{11}\,\beta_0^2 + 2\left(\beta_0 + \frac{13}{11}\,\beta_0^2\right)\frac{\xi_d(s;0)}{\xi_q(s;0)}\,, \tag{A6}$$

$$\Delta_{\psi 2}(s) = \frac{40}{11}\left(\beta_0 + \frac{1}{3}\,\beta_0^2\right) + 2\left(1 + \frac{50}{33}\,\beta_0 + \frac{13}{11}\,\beta_0^2\right)\frac{\xi_d(s;0)}{\xi_q(s;0)}\,, \tag{A7}$$

$$\Delta_{\psi 3}(s) = \beta_0^{-1} + 5 + \frac{25}{7}\,\beta_0 + \frac{1}{3}\,\beta_0^2 + \left(\beta_0^{-1} + \frac{19}{7} + \frac{61}{35}\,\beta_0 + \frac{19}{105}\,\beta_0^2\right)\frac{\xi_d(s;0)}{\xi_q(s;0)}\,. \tag{A8}$$

REFERENCES

Alcock, C., & Paczyński, B. 1979, Nature, 281, 358
Ballinger, W. E., Peacock, J. A., & Heavens, A. F. 1996, MNRAS, 282, 877
Bardeen, J. M., Bond, J. R., Kaiser, N., & Szalay, A. S. 1985, ApJ, 304, 15
Cole, S., Fisher, K. B., & Weinberg, D. H. 1994, MNRAS, 267, 785
———. 1995, MNRAS, 275, 515
Davis, M., & Peebles, P. J. E. 1983, ApJ, 267, 465
Fukugita, M., Shimasaku, K., & Ichikawa, T. 1995, PASP, 107, 945
Gunn, J. E., & Weinberg, D. H. 1995, in Wide Field Spectroscopy and the Distant Universe, ed. S. J. Maddox & A. Aragón-Salamanca (Singapore: World Scientific), 3
Hamilton, A. J. S. 1992, ApJ, 385, L5
Kaiser, N. 1987, MNRAS, 227, 1
Lahav, O, Lilje, P. B., Primack, J. R., & Rees, M. J. 1991, MNRAS, 251, 128
Loveday, J., Efstathiou, G., Maddox, S. J., & Peterson, B. A. 1996, ApJ, 468, 1
Loveday, J., Peterson, B. A., Efstathiou, G., & Maddox, S. J. 1992, ApJ, 390, 338
Magira, H., et al. 1998, in preparation
Matsubara, T., & Suto, Y. 1996, 470, L1
Peacock, J. A., & Dodds, S. J. 1994, MNRAS, 267, 1020
Peebles, P. J. E. 1980, The Large-Scale Structure of the Universe (Princeton: Princeton Univ. Press)
———. 1993, Principles of Physical Cosmology (Princeton: Princeton Univ. Press)
Ratcliffe, A., et al. 1996, MNRAS, 281, L47
Ryden, B. 1995, ApJ, 452, 25
Shectman, S. A., et al. 1996, ApJ, 470, 172
Strauss, M. A., & Willick, J. 1995, Phys. Rep., 261, 271